NUMERICAL METHOD FOR 3D COMPUTATION OF TURBOMACHINERY TONE NOISE

Anton ROSSIKHIN, Sergey PANKOV, Igor BRAILKO, Victor MILESHIN

*Central Institute of Aviation Motors (CIAM), 2 Aviamotornaya St.,
111116, Moscow, Russia*

SUMMARY

This paper presents the numerical method for 3D calculation of the turbomachinery tone noise generation, propagation and radiation in the near and far fields taking into account the interaction between rows. The method is built into CIAM domestic aeroacoustic solver 3DAS (3 Dimensional Acoustics Solver). Application of 3DAS solver for calculation of acoustic characteristics of a model ducted counter-rotating fan is described. The results of the computation are compared with the results of experiment.

INTRODUCTION

Fan noise generated by rotor-stator interaction is one of the major tone noise components of high-bypass ratio modern aeroengines [1]. To provide prediction capability for aeroengine noise the numerical method for 3D calculation of the turbomachinery tone noise generation, propagation and radiation in the near and far acoustic fields taking into account the interaction between rows is developed in CIAM. It is implemented in 3DAS (3 Dimensional Acoustics Solver) CIAM domestic solver. The method was used for calculations of acoustic characteristics of high bypass ratio fans of turbofan engines (single-rotating and counter-rotating), counter-rotating propellers and last stages of low pressure turbines [2,3].

First part of this paper contains description of the 3DAS solver. Strategy for the computation of turbomachinery tone noise in the far field is presented. Brief description of the numerical methods, used in the calculation is also provided.

Then application of 3DAS solver for calculation of acoustic characteristics of a model ducted counter-rotating fan is described. This type of fans is treated as a possible alternative for the conventional single-rotating fans in the high bypass ratio turbofan aviation engines. The fan under consideration was developed in the framework of European Project VITAL (EnVIronmenTALly friendlyaeroengine), and tested at the CIAM test rig facility [4]. We performed calculation of the forward tone noise of the fan in the operating mode correspondent to the certification point at approach conditions. The results of the computation were compared with the results of experiment at the same conditions.

3DAS SOLVER

The 3DAS solver is designed for the calculations of tone noise generation by the inter-row interaction in a turbomachine, tone noise propagation thought the duct of a turbomachine and tone noise radiation from the vicinity of a turbomachine to the far field.

The method of inter-row interaction calculation, implemented in 3DAS solver, is based on the solution of three-dimensional linear or nonlinear Euler equations for disturbances over viscous steady mean flow in the reference frames of blade rows. Interaction between blade rows of turbomachine is provided by so called "sliding grids" interface. They transfer unsteady acoustic (and also entropy and vorticity) disturbances and non-uniformities of mean steady flow field (for example rotor wakes) from one blade row to another. High order CAA (Computational Aero-Acoustics) numerical schemes for time and space discretization are used for the computation.

In its statement the method under consideration is close to the methods of inter-row interaction calculations based on unsteady Reynolds-Averaged Navies–Stokes (URANS) equations [5,6,7]. On the other side the usage of inviscid equations makes it more close to the methods of aft turbomachinery tone noise calculations, in which the response of the stator on the rotor's wakes (obtained in the independent RANS calculation) is considered [8,9,10]. Application of inviscid equations and high order CAA numerical schemes allows using relatively coarse grids.

In general 3DAS solver allows performing calculation of tone noise generation and propagation in one computation. However to simplify a problem and reduce calculation time we, as many authors from the aeroacoustic community [5,6,7,8,11], use hybrid approach, in which these problems are treated separately (though in our case with the same numerical methods). The results of the inter-row (rotor-stator or rotor-rotor) interaction calculation are used as input data for the propagation calculation.

The matching between the problems of interaction and propagation is organized [5], by decomposition of the perturbation field along a prescribed cross-section on acoustic modes in the coaxial cylindrical duct [12]. Outgoing acoustic modes found in the solution of the first problem are used as input data for the second one.

The problem of noise propagation calculation can be simplified if the duct is axisymmetric (which is the usual case for test rigs). In this case, the solution can be decomposed on axial harmonics, and calculation can be performed independently for each harmonic on two-dimensional domain correspondent to longitudinal section of initial three-dimensional geometry. In many cases the number of axial harmonics in the solutions is quite small, so the reduction of 3D problem to the set of 2D problems can lead to the saving of computational resources.

The method based on the Ffowcs-Williams and Hawkings equation with a penetrable data surface [13] is used to predict tone noise in the far field, using results of the calculations in the near field.

BRIEF DESCRIPTION OF THE CALCULATION METHOD

Governing equations

In the 3DAS aeoacoustic solver the system of Euler equations for disturbances over viscous steady mean flow is used to resolve the acoustic wave's generation and propagation in the turbomachines. The system of equation is derived from the Navier–Stokes equations under an assumption that the effects of viscosity and heat conduction normally control mean flow distribution rather than acoustic fluctuations. This assumption [11,14] is often used in aeroacoustics for calculation of noise

propagation in the nonuniform flow. Let us designate mean steady flow field variables by 0 and an unsteady fluctuation field by an apostrophe

$$\rho = \rho_0 + \rho', \ p = p_0 + p', \ v = v_0 + v', \ w = w_0 + w'.$$

Then, in a coordinate system rotating about the X axis with angular velocity Ω, we obtain [2]:

$$\frac{\partial \vec{U}'}{\partial t} + \frac{\partial \vec{E}'}{\partial x} + \frac{\partial \left[\vec{F}' - \Omega \cdot z \cdot \vec{U}' \right]}{\partial y} + \frac{\partial \left[\vec{G}' + \Omega \cdot y \cdot \vec{U}' \right]}{\partial z} = \vec{\Lambda} \qquad (1)$$

where:

$$\vec{U}'_1 = \begin{pmatrix} \rho' \\ \rho_0 \cdot u' + u_0 \cdot \rho' + u'\rho' \\ \rho_0 \cdot v' + v_0 \cdot \rho' + v'\rho' \\ \rho_0 \cdot w' + w_0 \cdot \rho' + v'\rho' \\ e' \end{pmatrix}$$

- nonlinear disturbance vector,

$$\vec{E}' = \begin{pmatrix} \rho_0 \cdot u' + u_0 \cdot \rho' + u' \cdot \rho' \\ 2 \cdot \rho_0 \cdot u_0 \cdot u' + u'^2 \cdot \rho_0 + u_0^2 \cdot \rho' + 2 \cdot \rho' \cdot u_0 \cdot u' + \\ \rho' \cdot u' \cdot u' + p' \\ \rho_0 \cdot u_0 \cdot v' + \rho_0 \cdot u' \cdot v_0 + \rho_0 \cdot u' \cdot v' + \rho' \cdot u_0 \cdot v_0 + \\ \rho' \cdot u' \cdot v_0 + \rho' \cdot u_0 \cdot v' + \rho' \cdot u' \cdot v' \\ \rho_0 \cdot u_0 \cdot w' + \rho_0 \cdot u' \cdot w_0 + \rho_0 \cdot u' \cdot w' + \rho' \cdot u_0 \cdot w_0 + \\ \rho' \cdot u' \cdot w_0 + \rho' \cdot u_0 \cdot w' + \rho' \cdot u' \cdot w' \\ (e_0 + p_0) \cdot u' + (e' + p') \cdot u_0 + (e' + p') \cdot u' \end{pmatrix}$$

- nonlinear flux in the X direction (nonlinear fluxes in the other directions $\vec{F}'$ and $\vec{G}'$ are determined similarly to $\vec{E}'$), and

$$\vec{\Lambda} = \begin{pmatrix} 0 \\ 0 \\ \Omega \cdot U_4' \\ -\Omega \cdot U_3' \\ 0 \end{pmatrix}$$

Energy disturbance e' is written in the following form:

$$e' = \frac{p'}{\gamma - 1} + (\rho_0 + \rho') \cdot (u_0 \cdot u' + v_0 \cdot v' + w_0 \cdot w') + \frac{1}{2} \cdot \rho' \cdot (u_0^2 + v_0^2 + w_0^2) + \frac{1}{2} \cdot \rho' \cdot (u'^2 + v'^2 + w'^2)$$

The mean flow variables can be easily obtained by calculating the Reynolds-Averaged Navies–Stokes equations (RANS) or Euler equations.

The system of linearized Euler equations (LEE), which is used in the 3DAS solver for calculation of acoustic disturbances propagation thru the duct, can be obtained from the system (1) by excluding the terms of the 2nd and higher orders.

The 3DAS solver is designed to use nonuniform nonorthogonal curvilinear grids. In the computational coordinates { $x = X(I,J,K)$, $y = Y(I,J,K)$, $z = Z(I,J,K)$ } the equation (1) takes the form:

$$\frac{\partial \vec{\psi}}{\partial t} + \frac{\partial \vec{A}}{\partial I} + \frac{\partial \vec{B}}{\partial J} + \frac{\partial \vec{C}}{\partial K} = \frac{\vec{\Lambda}}{\det(\Im)} \qquad (2)$$

where: $\psi = \vec{U}\,'/\det(\Im)$,

$$\vec{A} = \frac{1}{\det(\Im)}\left(\frac{\partial I}{\partial x} \cdot \vec{E}\,' + \frac{\partial I}{\partial y} \cdot \left[\vec{F}\,' - \omega \cdot z \cdot \vec{U}\,'\right] + \frac{\partial I}{\partial z} \cdot \left[\vec{G}\,' + \omega \cdot y \cdot \vec{U}\,'\right]\right)$$

Vectors $\vec{B}$ and $\vec{C}$ are determined similarly. Matrix $\Im$ is a Jacobi matrix, which is calculated numerically.

The inter-row interface

The calculation of interaction between rows in the time domain is based on the usage of sliding grid interfaces, similar to those used in [5]. The grids on the interfaces are connected one-to-one. The motion of the rotor relative to the stator (or other rotor) is accomplished by "sliding" the rotor grid system past the stator (other rotor) grid system. The interfaces transmit disturbances of the mean flow field (for example rotor wakes) from one grid to another in the form of disturbances of unsteady fluctuation values. Besides, the sliding grids interfaces provide transfer of unsteady disturbances from one block to another. Such an approach ensures the equality of overall parameters (mean flow + unsteady disturbances) on both sides of the grid boundaries. Our numerical studies show that interfaces correctly transfer acoustic waves and wakes from one grid system to the other, even if they have circumferential period less then 10 points. More detailed description of the interfaces with some examples can be found in [2] and [15].

The numeric method of solving the equation system

The input for our program is the steady mean flow field and the body-fitted computational grid. For turbomachinery tone noise applications the steady mean flow field in the blade rows is calculated in the "mixing-plane" approximation using RANS finite volume steady solvers of the second order.

The DRP (Dispersion-Relation-Preserving) approach proposed by K. Tam [16] was taken as a base of a spatial difference scheme used in our code. For convenience of the work with mean flow fields, provided by finite volume solvers, the scheme was generalized to the finite volume method (see [2] for details).

Second-order (fourth order in the linear case), four stages Runge-Kutta LDDRK (Low Dissipation and Dispersion Runge-Kutta Scheme) scheme (F. Hu et al. [17]) was used for time discretization.

To suppress high frequency spurious waves, artificial selective damping has been used, based on the fourth-order central filtering coefficients of O. Vasilyev [18]. In the solver are also implemented eight-order filtering coefficients, derived using the technique proposed by O. Vasilyev.

Boundary conditions

 The 3DAS solver includes several types of boundary conditions, which are defined on boundaries of blocks, constituting multi-block computational grid. In the present work were used the following types of boundary conditions:

- "Solid surface" boundary conditions - standard condition of non-leakage.

- "Inflow-outflow" boundary conditions. The one-dimensional characteristic boundary conditions [19,11] are used for the statement of boundary conditions of this type. In these boundary conditions the unsteady flow field on the boundary is decomposed on the ingoing and outgoing characteristic waves, and then ingoing waves are extracted from the solution. Usually these conditions are used with sponge layer.

- Boundary conditions with incoming disturbances of various types. These boundary conditions are based on characteristic boundary conditions. Let us denote $\hat{Z}$ as a matrix which extracts ingoing characteristic waves from the solution on the boundary $\vec{U}_b{}'$. Then the boundary conditions can be formulated as:

$$\vec{U} = \hat{Z}\left(\vec{U}_b{}' - \vec{U}_s{}'\right) + \vec{U}_s{}',$$

where $\vec{U}_s{}'$ is the field of the source. Numerical simulation shows that these boundary conditions accurately describe entrance of the incoming disturbances in the computational domain. However these boundary conditions are reflective, and in some cases can contaminate the solution.

- Boundary with an attached sub-domain. These conditions are specified by copying flow parameters from near-boundary cells to corresponding ghost cells of adjacent blocks.

- Periodic boundary conditions. These conditions organized by copying the flow parameters from the related near-boundary cells of the periodic boundary to the ghost boundary cells with subsequent turn of the velocity vector by an angle of periodicity.

Also to prevent unphysical reflections we use in our calculations buffer blocks in which grid cells are stretched near the outer boundaries [20]. In these blocks outgoing waves are absorbed by numerical viscosity. Usually the size of the grid cells near the outer boundary is set equal to the maximum wave length (in the direction normal to the boundary) of the waves expected in the solution. The size of the cells in the sponge layer changes from the region of fine grid resolution to the boundary according to the law of geometrical progression.

Modal analysis

In order to obtain sources to the problem of tone noise propagation through the inlet of engine, the results of the interaction calculation were decomposed at a series of outgoing acoustic modes in coaxial cylindrical channels [12]. Due to characteristic boundary conditions and special buffer zones we can assume, that disturbances on the surfaces of modal analysis correspond mostly to the outgoing radiation of the fan. So we can directly use obtained amplitudes and phases of acoustic modes for the specification of sources. More completely this method of matching between problem of generation and problem of propagation is described in [5].

Decomposition of the solution in terms of axial harmonics

The problem of noise propagation in the duct can be solved in the 3DAS solver by the same numerical method as the problem of noise generation. However the calculation can be simplified if the computational domain and the mean flow field have axial symmetry and the distortion can be characterized by a finite set of axial harmonics. Let us introduce in the calculation domain the curvilinear coordinates (I, J, K) of the form: $X = f_1(I,J)$, $Y = f_2(I,J)\cos(aK)$, $Z = f_2(I,J)\sin(aK)$.

In this case we can reduce linearized Euler equations to the set of independent equations for axial harmonics of the field. Physical variables at each point can be expanded in terms of time and polar angle into Fourier series. For scalar and vector variables we have correspondingly

$$f = \sum_{mn} f_{mn}(I,J)e^{-i\omega_n t + imaK}$$

$$\vec{f} = \sum_{mn} \left(\vec{n}_x f_{x\ mn}(I,J) + \vec{n}_r f_{r\ mn}(I,J) + \vec{n}_\varphi f_{\varphi\ mn}(I,J) \right) e^{-i\omega_n t + imaK}$$

where $\vec{n}_x$, $\vec{n}_r$ and $\vec{n}_\varphi$ are the orts of cylindrical system of coordinates.

Let us define $\vec{U}_l{}'_{mn}(I,J)$ - the field of the m-th axial harmonic with frequency ω_n on the $K = 0$ plane (l subscript denotes linearization). Then in the frequency domain we obtain from (2):

$$\frac{\partial \vec{A}_{l\ mn}}{\partial I} + \frac{\partial \vec{B}_{l\ mn}}{\partial J} = \frac{1}{\det(\Im)} \left(-O_m \vec{C}_{l\ mn} + \vec{\Lambda}_{l\ mn} + i \cdot \omega_n \cdot \vec{U}_l{}'_{mn} \right) \qquad (3)$$

where matrix $O_{m\ ij} = im\delta_{ij} + a(\delta_{i4}\delta_{j3} - \delta_{i3}\delta_{j4})$ in tensor notation.

To solve the obtained system of equation we use in our solver the pseudotime relaxation method with the local time step [21]. Our estimation showed, that for approximately uniform grid, the reduction of the 3D problem to a set of 2D ones is favorable when number of axial modes is less than circumferential dimension of the 3D grid divided on three. However for inlet grids with singularity on the axis, and correspondingly, global time step, determined by the small cells near the axis, the advance in performance can be much more.

Ffowcs Williams method for computation of acoustic disturbances in the far field

In the 3DAS solver acoustic near field from the vicinity of the nacelle is extrapolated to the far field using method based on Ffowcs Williams and Hawkings equation with a penetrable data surface. As it is well known [13] the solution of the Ffowcs Williams equation for the field in the external domain of the moving surface can be presented as the sum of three components:

$$p'(\mathbf{x},t) = p'_T(\mathbf{x},t) + p'_L(\mathbf{x},t) + p'_Q(\mathbf{x},t)$$

where p'_T, p'_L and p'_Q - monopole, dipole and quadrupole contributors to radiation. The first two components depend from field variables on the surface while the third term is volumetric. Fortunately, usually the surface of integration (data surface) can be chosen in such a way to get a negligible contribution to radiation from the quadrupole source (in our case – sufficiently far from the lips of inlet). Therefore, we can limit our analysis to the first two contributions.

Let's first introduce two variables - U_i and L_i:

$$U_i = \left[1 - \frac{\rho}{\overline{\rho}} \right] v_i + \frac{\rho u_i}{\overline{\rho}}, \quad L_i = P_{ij}\hat{n}_j + \rho u_i \left(u_j - v_j \right)\hat{n}_j$$

Here $\hat{n}_i$ - unit vector which is normal to the surface, u_i - flow velocity, v_i - surface velocity and $\overline{p}$ and $\overline{\rho}$ - are respectively pressure and density of steady flow at a large distance from the surface.

In terms of these variables we can write out [13]:

$$4\pi p'_T(\mathbf{x},t) = \int_S \left[\frac{\overline{\rho}\dot{U}_j\hat{n}_j}{r(1-M_r)^2} + \frac{\overline{\rho}U_j\hat{n}_j(r\dot{M}_r + \overline{c}(M_r - M^2))}{r^2(1-M_r)^3} \right]_{\tau=\tau_{ret}} dS$$

$$4\pi p'_L(\mathbf{x},t) = \int_S \left[\frac{\dot{L}_j\hat{r}_j}{\overline{c}r(1-M_r)^2} + \frac{L_j\hat{r}_j - L_j M_j}{r^2(1-M_r)^2} \right]_{\tau=\tau_{ret}} dS + \frac{1}{\overline{c}} \int_S \left[\frac{L_j\hat{r}_j(r\dot{M}_r + \overline{c}(M_r - M^2))}{r^2(1-M_r)^3} \right]_{\tau=\tau_{ret}} dS$$

In these expressions $\overline{c}$ - sound speed in steady uniform flow, $M_r \equiv M_j \hat{r}_j$, where $M_j = v_j/\overline{c}$ and $\hat{r}$ - unit vector along r. Surface emission times τ_{ret} for each point of the surface are found by solving following equation $-\tau - t + r(\tau)/\overline{c} = 0$.

The method under study is integrated into CIAM's solver 3DAS and can be used both in time and in frequency domains (for axial harmonics). Integration on the surface is made by numerical methods of the second accuracy order.

3D SIMULATION OF FORWARD TONE NOISE OF COUNTER-ROTATING DUCTED FAN

In this paper application of our method for calculation of tone noise generation, propagation and radiation is illustrated on the example of 3D simulation of forward noise of a counter-rotated ducted fan (fig. 1). The number of the first rotor blades for this fan is 10, the number of the second rotor blades is 14. The fan diameter is D=0.56 m. Flight configuration considered is the certification point at aircraft approach conditions.
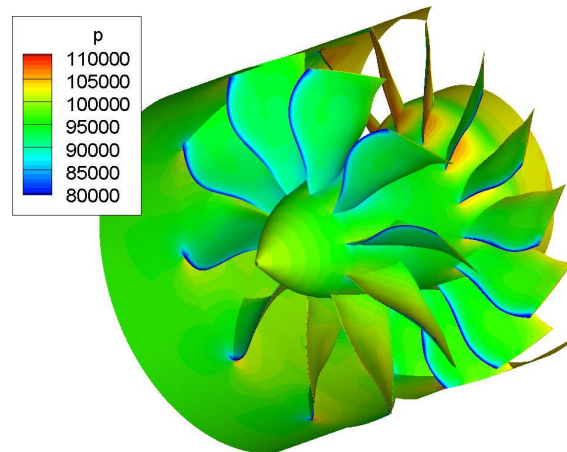
Figure 1: Counter-rotating fan. Field of steady static
pressure on the blades and the case

The first stage of the simulation was the computation of mean steady flow fields using RANS equations, the semi-empirical model of turbulence, and "mixing-plane" interfaces between blade rows. It was performed with one of the CIAM domestic aerodynamic solvers "3D-IMP_MULTI" [2]. To simplify the problem calculation was performed with zero tip clearance. Additional information about steady flow computations can be found in [22].

Second stage, was the computation of tone noise of rotor-rotor interaction using nonlinear Euler equation for disturbances. The longitudinal section of the grid for the unsteady computation and its magnified fragment are shown in fig. 2. The grid is derived from the grid for the steady flow field calculations and contains 5 interblade channels for the first rotor and 7 for the second. To avoid unphysical reflections from the boundaries we added buffer zones to the calculation region in front and behind the fan (shown on fig. 2 in blue). Fig. 3 shows the unsteady field of static pressure (mean flow + pulsations) on the radial section of fan channel. In fig. 4 is shown the unsteady field of entropy function P/ρ^γ. We see, that interfaces correctly transfer (back and forth) the wake disturbances obtained in the steady computation from grid blocks related to the coordinate system of the first rotor to the blocks related to coordinate system of the second rotor.
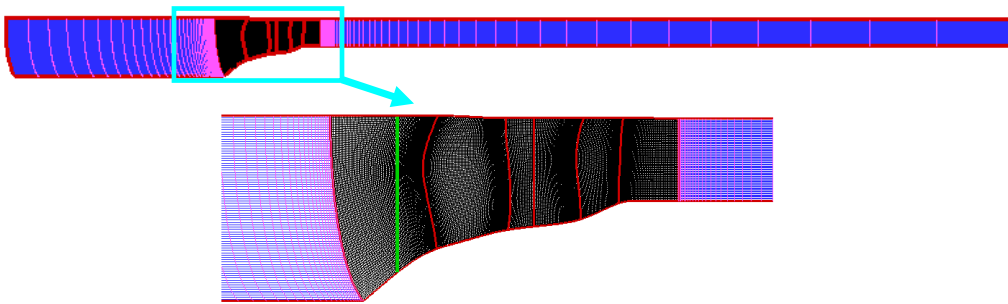
Figure 2: The grid for the unsteady calculation
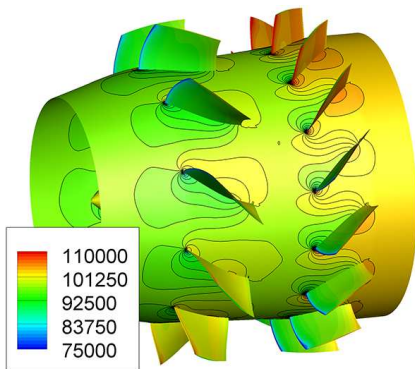
Figure 3: Unsteady static pressure field
(mean flow + pulsations)
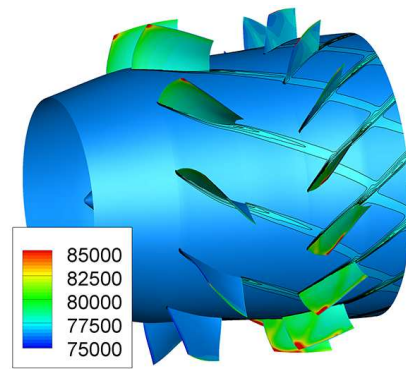
Figure 4: Unsteady field of entropy function
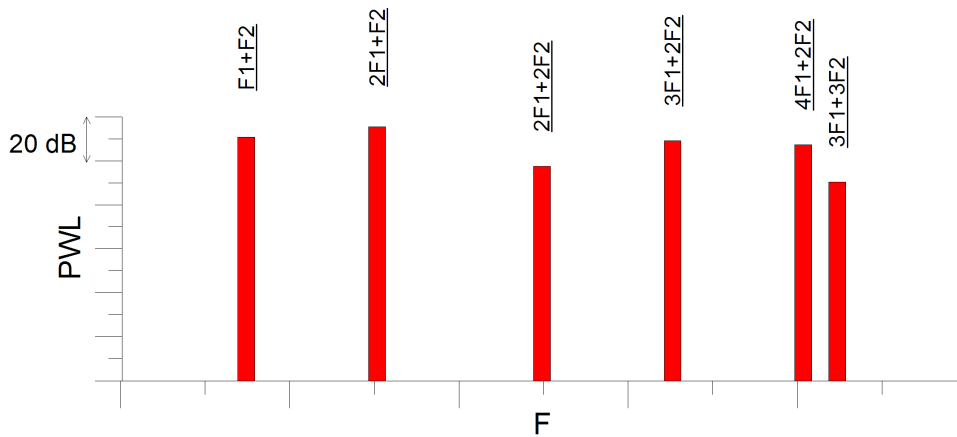
Figure 5: The intensities of tone noise harmonics, corresponding
to propagating acoustic modes.

During the final stage of rotor-rotor interaction computation, the unsteady flow field quantities data were collected on surface in the fan inlet (colored in green in fig. 2). On this surface we performed mode decomposition, to find sources for computation of tone noise radiation from the inlet. They were specified as a set of acoustic modes in the coaxial cylindrical duct. Sources were calculated for frequencies below and equal to $3F_1+3F_2$, where $F_1=10N_1$ is the blades passage frequency of the first rotor, and $F_2=14N_2$ – blades passage frequency of the second rotor (N_1 and N_2 – rotation frequencies of the first and second rows). The power levels of the most intensive tone noise harmonics in the specified frequency range are shown in fig. 5. It is known [5-8,12], that acoustic modes, generated by rotor-rotor interaction must satisfy special conditions on frequencies and

circumferential orders. Outgoing modes deduced from the unsteady solution in our case were found to be in complete agreement with the modes expected from the theory of interaction.

Table 1: Frequencies and circumferential orders of acoustic modes, generated by the fan

Harmonic	F1+F2	2F1+F2	2F1+2F2	3F1+2F2	4F1+2F2	3F1+3F2
m	4	-6	8	-2	-12	12

Based on the results of the modal decomposition, the calculation of tone noise propagation through the inlet of the fan was performed. CIAM's 3DFS solver [2] was used for computation of the mean steady flow field in the inlet. Calculation domain and the results of the calculation for Mach number field are represented in fig. 6. Noise propagation was computed using linearized Euler's equations for axial harmonics (3) in the frequency domain. In our case all interaction modes with the same frequency have equal circumferential order (see Table 1). So in the frequency range specified we had to perform six calculations. In fig. 7 is shown real part of static pressure pulsations in the inlet for harmonic $4F_1+2F_2$ (presented fragment of computational domain nearly corresponds to the region of fine grid – other parts of the domain belong to sponge layer).
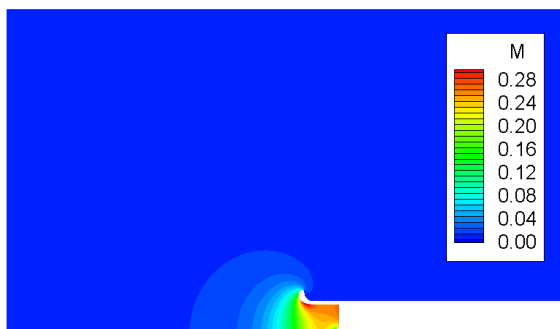
Figure 6: Steady Mach number field in the inlet
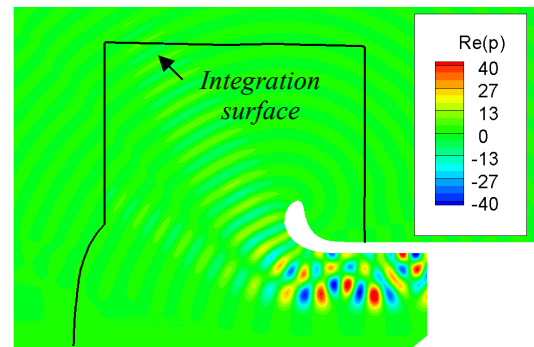
Figure 7: Real part of static pressure pulsations in the inlet
(F = 4F$_1$+2F$_2$, m = -12)
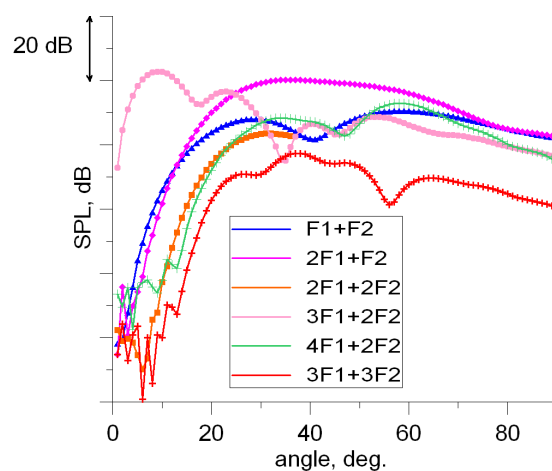
Figure 8: Directivity diagrams of sound pressure level for harmonics under consideration

To compute fan tone noise radiation in the far field Ffowcs Williams method was used. Black line in fig. 7 shows position of the integration surface. Pressure pulsations were computed at points

placed along the arc with r= 4 m and the center in the central point of the inlet section with uniform angular distribution within 1-90° with 1° spacing. The directivity diagrams of sound pressure level SPL (dB) for all six harmonics are shown in fig. 8.
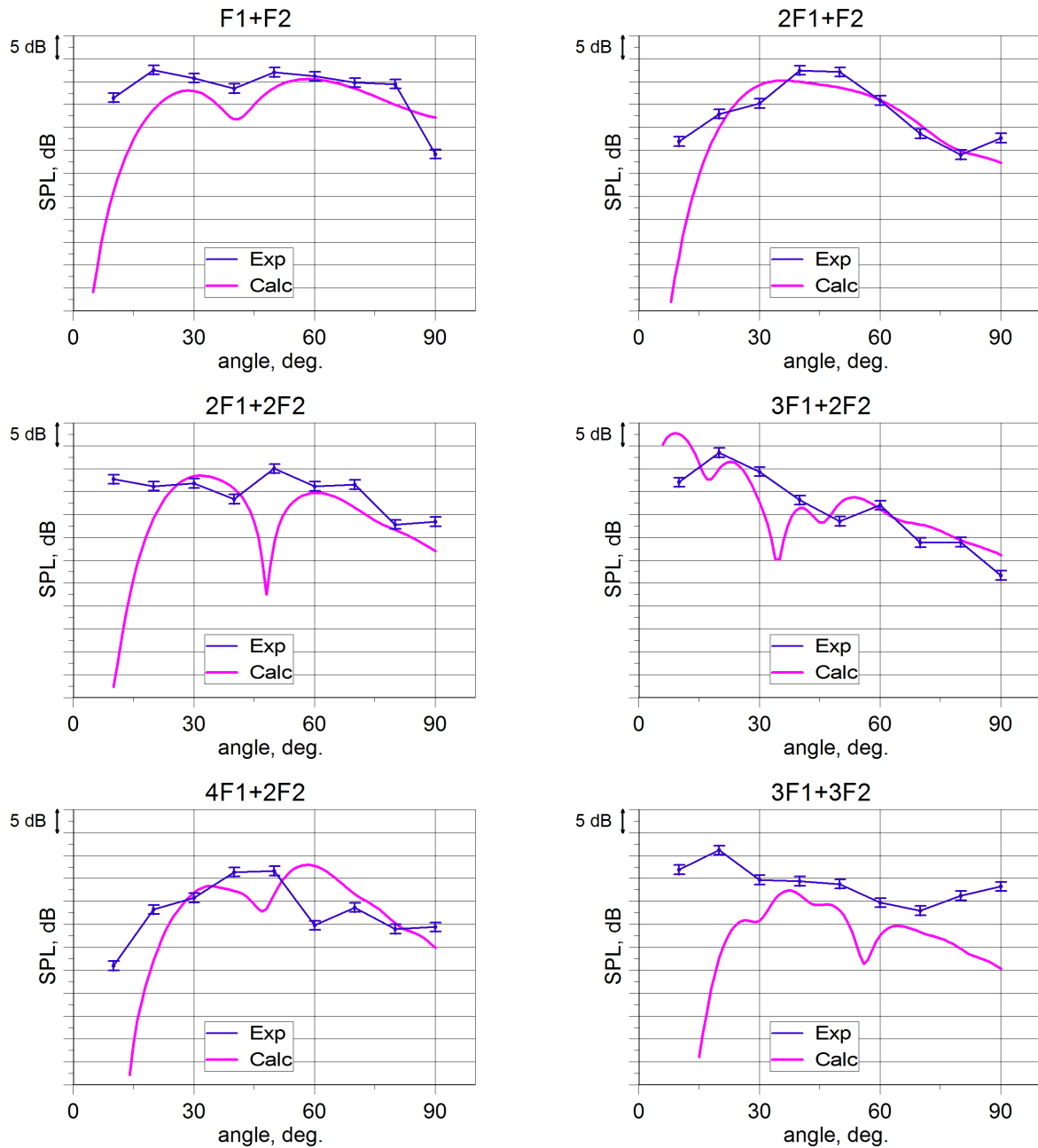
Figure 9: Directivity diagrams of sound pressure level for most intensive tones in the far field
(calculation and experiment)

The results of the simulation in the far field were compared with the results of the experiment for the same fan on the CIAM test rig C-3A [4]. The results of comparison are showed in fig. 9. We see satisfactory qualitative and, in some positions of microphones, quantitative agreement between the results of the simulation and the experiment, except for the harmonics $3F_1+3F_2$. However for the last harmonic levels of tone noise in the experiment lay below the levels of broadband noise. So their real intensity can not be derived from narrowband spectrum with good precision. Also the frequency of this harmonic lays only 10% below our estimation of the maximum frequency

resolved in the rotor-rotor interaction calculation, which can also be important. Another noticeable feature is the significant difference between the calculation and the experiment for angle position of microphone 10°. This result can be explained by insufficient resolution of the computational grid for inlet near the inlet axis. On the other side for microphones with angle positions 60° and 80 we see good correspondence between the calculation and the experiment for four harmonics out of six.

Qualitative comparison with the far field noise simulation results for the same fan, published in [6], shows significant difference between our results and the results of ONERA in the forms of directivity diagrams. Comparison with other works devoted to the far field directivity data assessment [8] for single rotating fans shows comparable accuracy of results.

CONCLUSION

The numerical method for 3D calculation of the turbomachinery tone noise generation, propagation and radiation in the near and far fields taking into account the interaction between rows has been presented. Application of this method for the calculation of acoustic characteristics of a model ducted counter-rotating fan has been demonstrated. Outgoing acoustic modes deduced from unsteady solution on an input in the fan were found to be in agreement with interaction modes expected from theory. Comparison with the experiment showed satisfactory qualitative and in some positions of microphones quantitative agreement between the results of the simulation and the experiment for the first five interaction harmonics.

The next step will be to perform computation of tone noise for another certification points. Also it is planned to perform assessment for another counter-rotating fans developed in the framework of the VITAL project.

BIBLIOGRAPHY

[1]   H.H. Hubbard (ed.) - *Aeroacoustics of Flight Vehicles: Theory and Practice, Volume 1: Noise Sources*, NASA-RP-1258-Vol-1, **1991**

[2]   Nyukhtikiv M., Brailko I., Mileshin V., Pankov S. – *Computational and Experimental Investigation of Unsteady and Acoustic Characteristics of Counter – Rotating Fans*, HT-FED2004-56435, Proceedings of 2004 ASME Heat Transfer / Fluids engineering Summer Conference, Charlotte, North Carolina USA, July 11-15, **2004**

[3]   Nyukhtikov M.A., Rossikhin A.A., Sgadlev V.V., Brailko I.A. – *Numerical Method for Turbo-Machinery Tonal Noise Generation and Radiation Simulation Using CAA Approach*, GT2008-51182, Proceedings of ASME Turbo Expo 2008: Power for Land, Sea and Air, GT2008, Berlin, Germany June 9-13, **2008**

[4]   Khaletskiy Y., Mileshin V., Shipov R. – *Acoustic Test Facility for Aero Engine Fans*, Proceeding of the International Forum "Acoustics'08 – EuroNoise", pp. 587-590, Paris, France, June 29- July 4, **2008**

[5]   Rumsey C. L., Biedron R. T., Farassat F. – *Ducted-Fan Engine Acoustic Predictions Using a Navier-Stokes Code*, Journal of Sound and Vibration, Vol. 213, No. 4, pp. 643-664, **1998**

[6]   Polacsek C., Barrier R. – *Numerical Simulation of Counter-Rotating Fan Aeroacoustics*, AIAA 2007-3680, 13th AIAA/CEAS Aeroacoustics Conference, Rome, Italia, May 20-23, **2007**

[7]   Weckmüller C., Guerin S., Ashcroft G. – *CFD-CAA Coupling Applied to DLR UHBR-Fan: Comparison to Experimental Data,* AIAA 2009-3342, Miami, Florida, May 11-13, **2009**.

[8]   Nark D. M., Envia E., Burley C. L. – *Fan Noise Prediction with Applications to Aircraft System Noise Assessment,* AIAA-2009-3291, 15th AIAA/CEAS Aeroacoustics Conference, Miami, Florida, May 11-13, **2009**

[9]   Sharma A., Richards S. K., Wood T. H., Shieh C. – *Numerical Prediction of Exhaust Fan-Tone Noise from High-Bypass Aircraft Engines*, AIAA Journal, Vol. 47, No. 12, pp. 2866-2878, **2009**

[10]   Ray Hixon, Adrian Sescu, Scott Sawyer – *Votrical Gust Boundary Conditions for Realistic Rotor Wake/Stator Interaction Noise Prediction Using Computational Aeroacoustics*, Journal of Sound and Vibration, Vol. 330, No. 16, pp. 3801-3817, **2011**

[11]   Dierke J., Ewert R., Chappuis J., Lidoine S., Ricouard J. – *The Influence of Realistic 3D Viscous Mean Flow on Shielding of Engine-Fan Noise by a 3-Element High-Lift Wing*, AIAA 2010-3917, 16th AIAA/CEAS Aeroacoustics Conference, Stockholm, Sweden, June 7-9, **2010**

[12]   Tyler J.M., Sofrin T.G. – *Axial Flow Compressor Noise Studies*, SAE Transactions, Vol. 70, pp. 309–332, **1962**

[13]   Brentner K.S., Farassat F. – *Analytical Comparison of the Acoustic Analogy and Kirchhoff Formulation for Moving Surfaces*, AIAA Journal, Vol. 36, No. 8, pp. 1379–1386, **1998**

[14]   Shen W.Z., Sorensen J.N. – *Aeroacoustic Modelling of Low-Speed Flows*, Theoret. Comput. Fluid Dynamics, Vol. 13, pp. 271-289, **1999**

[15]   Nyukhtikov M.A., Rossikhin A.A. – *Numerical Method for Calculating Three-Dimensional Fan Tonal Noise Due to Rotor-Stator Interaction*, Proceedings of International Congress «Turbomachines: Aeroelasticity, Aeroacoustics, and Unsteady Aerodynemics» – Moscow: TORUS PRESS Ltd., pp. 268-280, **2006**.

[16]   Tam C.K.W., Webb J.C. – *Dispersion-Relation-Preserving Schemes for Computational Acoustics*, Journal of Computational Physics, Vol. 107, pp. 262-281, **1993**

[17]   Hu F.Q., Hussaini M.Y., Manthey J. – *Low-Dissipation and Low-Dispersion Runge-Kutta Schemes for Computational Acoustics,* Journal of Computational Physics, Vol. 124, pp. 177-191, **1996**

[18]   Vasilyev O. – *A General Class of Commutative Filters for LES in Complex Geometries*, Journal of Computational Physics, Vol. 146, pp. 82–104, **1998**

[19]   Giles M.B. – *Nonreflecting Boundary Conditions for Euler Equation Calculations*, AIAA Journal, Vol. 28, No. 12, pp. 2050–2058, **1990**

[20]   Efraimsson G. Biela C. – *Analysis of Aeroacoustic Wave Propagation Simulations Using a Higher-Order Accurate Method*, AIAA 2006-2471, 12th AIAA/CEAS Aeroacoustics Conference, Cambridge, Massachusetts, May 8-10, **2006**

[21]   McMullen M., Jameson A., Alonso J. – *Acceleration of Convergence to a Periodic Steady State in Turbomachinery Flows*, AIAA 2001-0152, 39th AIAA Aerospace Sciences Meeting & Exhibit, Reno, NV, January 8-11, **2001**

[22]   Mileshin V., Orekhov I., Pankov S. – *Numerical And Experimental Investigations of Single-Flow and Bypass-Flow Fans*, Paper 039, International Conference Fan 2012, Senlis, France, April 18-20, **2012**